Title

Ancient European dog genomes reveal continuity since the early Neolithic

Authors

Laura R. Botigué[1,†], Shiya Song[2,†], Amelie Scheu[3,8,†], Shyamalika Gopalan[1], Amanda L. Pendleton[4], Matthew Oetjens[4], Angela M. Taravella[4], Timo Seregély[5], Andrea Zeeb-Lanz[6], Rose-Marie Arbogast[7], Dean Bobo[1], Kevin Daly[8], Martina Unterländer[3], Joachim Burger[3], Jeffrey M. Kidd[2,4], Krishna R. Veeramah[1,*]

Affiliations

[1] Department of Ecology and Evolution, Stony Brook University, Stony Brook, New York, 11794-5245, USA.

[2] Department of Computational Medicine and Bioinformatics, University of Michigan, Ann Arbor, MI 48109, USA.

[3] Palaeogenetics Group, Johannes Gutenberg-University Mainz, 55099 Mainz, Germany.

[4] Department of Human Genetics, University of Michigan, Ann Arbor, MI 48109, USA.

[5] Department of Prehistoric Archaeology, Institute of Archaeology, Heritage Sciences and Art History, University of Bamberg, 96045 Bamberg, Germany.

[6] Generaldirektion Kulturelles Erbe Rheinland-Pfalz, State Archaeology, Department for Monumental Heritage Speyer, 67346 Speyer, Germany.

[7] CNRS UMR 7044-UDS, 5 allée du Général Rouvillois F 67083 Strasbourg, France.

[8] Smurfit Institute of Genetics, Trinity College Dublin, Dublin 2, Ireland.

†These authors contributed equally to this work

*corresponding author: krishna.veeramah@stonybrook.edu

Keywords

Ancient DNA, dog domestication, Neolithic, Europe

Abstract

Europe has played a major role in dog evolution, harbouring the oldest uncontested Palaeolithic remains and having been the centre of modern dog breed creation. We sequenced the whole genomes of an Early and End Neolithic dog from Germany, including a sample associated with one of Europe's earliest farming communities. Both dogs demonstrate continuity with each other and predominantly share ancestry with modern European dogs, contradicting a Late Neolithic population replacement previously suggested by analysis of mitochondrial DNA and a Late Neolithic Irish genome. However, our End Neolithic sample possesses additional ancestry found in modern Indian dogs, which we speculate may be derived from dogs that accompanied humans from the Eastern European steppe migrating into Central Europe. By calibrating the mutation rate using our oldest dog, we narrow the timing of dog domestication to 20,000-40,000 years ago. Interestingly, the extreme copy number expansion of the *AMY2B* gene found in modern dogs was not observed in the ancient samples, indicating that the *AMY2B* copy number increase arose as an adaptation to starch-rich diets after the advent of agriculture in the Neolithic period.

Introduction

Europe has been a critically important region in the history and evolution of dogs, with most modern breeds having a common European ancestry (Parker et al. 2004). Furthermore, the oldest remains that can be unequivocally attributed to domestic dogs (*Canis lupus familiaris*) are found on the continent, including an Upper Paleolithic 14,700-year-old jaw-bone from the Bonn-Oberkassel site in Germany (Benecke 1987), and although older specimens from Siberia and the Near East have been proposed, these are highly controversial (Perri 2016; Horard-Herbin et al. 2014). Analysis of mitochondrial and genomic data from modern dogs have suggested East Asia (Savolainen et al. 2002; Wang et al. 2016), the Middle East (Vonholdt et al. 2010) and Central Asia (Shannon et al. 2015) all as potential centers of dog domestication. However, ancient mitochondrial DNA (mtDNA) points to a possible European origin (Thalmann et al. 2013).

The Neolithic period in Central Europe ranges from ~5,500-2,000 cal BCE and can be further subdivided based on aspects of human culture (Supplementary Methods 1). Intriguingly, multiple studies have found evidence of a striking prehistoric turnover of mtDNA lineages in the European continent sometime between the Late Neolithic and today, with haplogroup C, which

appears in almost all Neolithic dogs but less than 10% of modern dogs, being replaced by haplogroup A in most of Europe (Deguilloux et al. 2009; Frantz et al. 2016; Thalmann et al. 2013). Frantz et al. (Frantz et al. 2016) argue that this matrilineal turnover was a consequence of a population replacement by analyzing genomic data from modern dogs as well as a Late Neolithic (~5,000 years) Irish dog from Newgrange (henceforth referred to as NGD). Placing their results within the context of existing archaeological data, they also posited a novel dual origin for domestication. However, NGD shares ancestry primarily with modern European dogs, implying the proposed population replacement had largely already occurred by this time.

The characterization of samples from earlier in the Neolithic and from continental Europe are therefore necessary to examine whether and to what extent a large-scale replacement occurred on the continent during this period, which would be evidenced by the presence of a distinct ancestry not present in modern dog genomes, as opposed to genomic continuity from the Early Neolithic to today. This, in turn, is key for understanding human-dog interactions during the major replacement of indigenous Paleolithic hunter-gatherers by Neolithic farmers from Anatolia (Bramanti et al. 2009; Hofmanová et al. 2016), and the subsequent migrations from the Eastern European steppe (Haak et al. 2015), as well as for disentangling the process of dog domestication.

We present analysis of ~9x coverage whole genomes of two dog samples from Germany dating to the Early and End Neolithic (Supplementary Methods 1-4) and demonstrate genetic continuity throughout this era as well as substantial shared ancestry with modern European dogs. However, we also find that the End Neolithic sample possesses an additional ancestry component consistent with admixture from a population of dogs found further east which may have migrated concomitant with people originating from the steppe associated with Late Neolithic and Early Bronze age cultures, such as Yamnaya and Corded Ware. We also show that most autosomal haplotypes previously associated with domestication were already established in our Neolithic dogs, though adaptation to a starch-rich diet likely occurred later. Our results are consistent with a single domestication process that occurred between ~20,000-40,000 years ago.

Results

Archaeological samples and Ancient DNA sequencing

The older specimen (and the oldest whole nuclear genome sequenced dog to date), which we refer to hereafter as HXH, was found at the Early Neolithic site of Herxheim and is dated to 5,223-5,040 cal. BCE (~7,000 years old) (Supplementary Figure S1.2.1). The younger specimen, which we refer to hereafter as CTC, was found in the Kirschbaumhöhle (Cherry Tree Cave) and is dated to 2,900-2,632 cal. BCE (~4,700 years old), which corresponds to the End Neolithic period in Central Europe (Seregély et al. 2015) (Supplementary Figure S1.3.1).

We generated paired-end Illumina whole-genome sequencing data for the two ancient dog samples and successfully mapped over 67% of the reads to the dog reference genome (CanFam3.1), confirming high endogenous canine DNA content for both samples (Supplementary Methods 4). MapDamage (Ginolhac et al. 2011) analysis demonstrated that both samples possessed characteristics typical of ancient DNA (Briggs et al. 2007) such as high numbers of 5' C>T and 3' G>A changes at the end of fragments (~35% and 28% of each transition category for HXH and CTC, respectively), while fragment length was also small (mean 60-70bp) (Supplementary Figure S4.1.1). We examined potential human contamination by mapping a subset of ~1 million random reads to the hg19 reference genome. Only ~3% of reads mapped to the human genome for both samples, and almost all of these reads also mapped to CanFam3.1, which indicated very low levels of human contamination in our data. Overall, we conclude that both our samples appear to contain substantial authentic canine ancient DNA. The final mean coverage for both samples was ~9x. Additionally, the mean coverage for the X and Y chromosomes was ~5x for both samples, indicating they are males. In addition, we reprocessed the NGD data using the same pipeline and reference genome as for CTC and HXH.

Standard genotype callers such as the GATK Unified genotyper are targeted to the processing of modern genomes, and post-mortem damage in ancient DNA can affect their performance. We thus used a custom genotype caller implemented in Python (see Methods) that incorporates DNA damage patterns estimated from MapDamage using the likelihood model described in (Hofmanová et al. 2016). Additionally, any site with less than 7x coverage was reported as missing. Finally, any position where the highest likelihood is a heterozygote must have a minimum Phred-scaled genotype quality of 30 or the next highest homozygote likelihood genotype was chosen instead. We found that this practice eliminated many false positives that are the likely result of post-mortem damage, resulting in much more balanced numbers of C>T

vs T>C and G>A vs A>G heterozygous reference to alternate allele changes compared to when using the standard GATK Unified Genotyper caller (Supplementary Figure S5.1.2) (however, we note that when a site is already known to be segregating in other dogs or wolves, our algorithm and GATK Unified Genotyper are almost completely concordant for sites with >7x coverage). The balance was slightly improved for CTC compared to HXH, presumably as post-mortem damage is less extensive for the former. Despite its high mean coverage (~28x), balance was also noticeably improved when applying this SNP calling framework for NGD. The transition/transversion ratio was only slightly less than other modern canid genomes for CTC and HXH, while NGD, concomitant with its increased coverage, was clustered within the modern canid genomes (Supplementary Figures S5.1.3-4)

Modern Canid Reference Datasets

In order to better understand how these Neolithic dogs are genetically related to modern dogs, we analyzed them within the context of a comprehensive collection of 5,649 canids, including breed dogs, village dogs and wolves previously genotyped at 128,743 SNPs (Shannon et al. 2015; Pilot et al. 2015), as well as 99 canid whole genomes sequenced at medium to high coverage (6-45x), including NGD.

We explored different ascertainment schemes for the whole genome data (Supplementary Methods 6.2). In each case, variant sites on the autosomes were identified in specific sets of individuals and then genotyped across all sequenced samples. Call set 1 includes variants discovered in 89 contemporary genomes for which we processed the sequencing reads, the 3 ancient genomes and 6 genomes obtained from the Freedman et al. (Freedman et al. 2014) call set based on Illumina and SOLiD data. This call set represents the most comprehensive set of variants, but may show biases due to differences in coverage among sample sets. Call set 2 only includes variants discovered in the three ancient genomes. Call set 3 only includes sites discovered as variable in New World wolves. This call set contains 1,815,911 variants which must either be private to New World Wolves or arose in the Gray Wolf (*Canis lupus*) ancestral population, and thus is the least biased with regard to their ascertainment in Old World wolves and dogs. We note that gene flow between New World wolves and Old World canids could potentially bias the observed genetic variation in this call set. However, previous genomic studies have reported very low to negligible migration rates only between Mexican wolves and Basenji/Dingo (Fan et al. 2016) and analysis of one locus under positive selection that confers

black coat color suggests a potential old introgression from dogs to North American wolves (though we note that selection on standing variation cannot be ruled out) (Anderson et al. 2009). In both cases these admixture events should have minimal impact on our analyses which primarily involve Eurasian dogs.

We performed Principal Component Analysis (PCA) on the three call sets to explore how the possible biases in each might differentially affect the genetic differentiation observed in our data (Supplementary Methods 8). When we include all canids we observe that in call sets 2 and 3 genetic differentiation across dogs is already reflected in PC2, whereas all dogs cluster together in that PC in call set 1 (Supplementary Figures S8.1.3-5). However, when we only include dogs and remove groups used for ascertainment, the three call sets are consistent with the pattern observed in a PCA performed using the SNP array data, suggesting that the patterns of genetic differentiation amongst samples are robust across the different ascertainment schemes (Supplementary Figures S8.1.6-8). Additionally, we explored the effect that potentially damaged bases (C > T and G > A transitions) could have in downstream analyses by performing a PCA on the SNP array dataset (Supplementary Figure S8.1.1) including our ancient samples with and without transitions. We found that the relative position of the three ancient samples was essentially unaffected, further validating our ancient DNA calling method for known SNP positions. Therefore, transitions were included in all subsequent SNP-based analyses. Although PCA reveals that the three call sets broadly capture the same variation patterns, we cannot control bias related to differences in coverage from call set 1 (which includes higher-coverage breed dogs) and cannot reliably identify false variation in call set 2 as a consequence of post-mortem damage. We therefore utilize call set 3, with variants ascertained in New World wolves, as the primary call set for most analyses.

Mitochondrial DNA analysis

We examined the phylogenetic relationship of the entire mitochondrial genomes of HXH and CTC with a comprehensive panel of modern dogs across four major clades (A-D), modern wolves and coyotes, and previously reported (Frantz et al. 2016; Thalmann et al. 2013) ancient wolf-like and dog-like whole mitochondrial sequences. Like other European Neolithic dogs examined previously, both HXH and CTC belong to haplogroup C (Figure 1A and Supplementary Methods 7), together with NGD and the Upper Paleolithic 12,500 year old Kartstein Cave dog (also from Germany). We note that Bonn-Oberkassel also falls in the same

haplogroup (Thalmann et al. 2013) (although analysis of this sample is complicated by low mtDNA sequence coverage, see Supplementary Methods 7), pointing to some degree of matrilineal continuity in Europe over at least ~10,000 years, ranging from the late Paleolithic to almost the entire Neolithic. The inclusion of 24 additional clade C samples (Duleba et al. 2015) in the phylogenetic analysis reveals the expected C1 and C2 split (100% support) and that HXH, CTC, NGD and the ancient German dog share a common lineage with C1 dogs (Supplementary Figure S7.2.2). This topology suggests that these ancient dogs in Europe belong to an older, novel sub-haplogroup that is sister to the progenitor of the C1b and C1a sub-haplogroups and possibly non-extant in modern dog populations. Incorporation of additional whole mtDNA sequences, from both ancient and modern dogs, will allow for the determination of whether this sub-haplogroup lineage has gone extinct in Europe or is simply undetected in our current sample set.

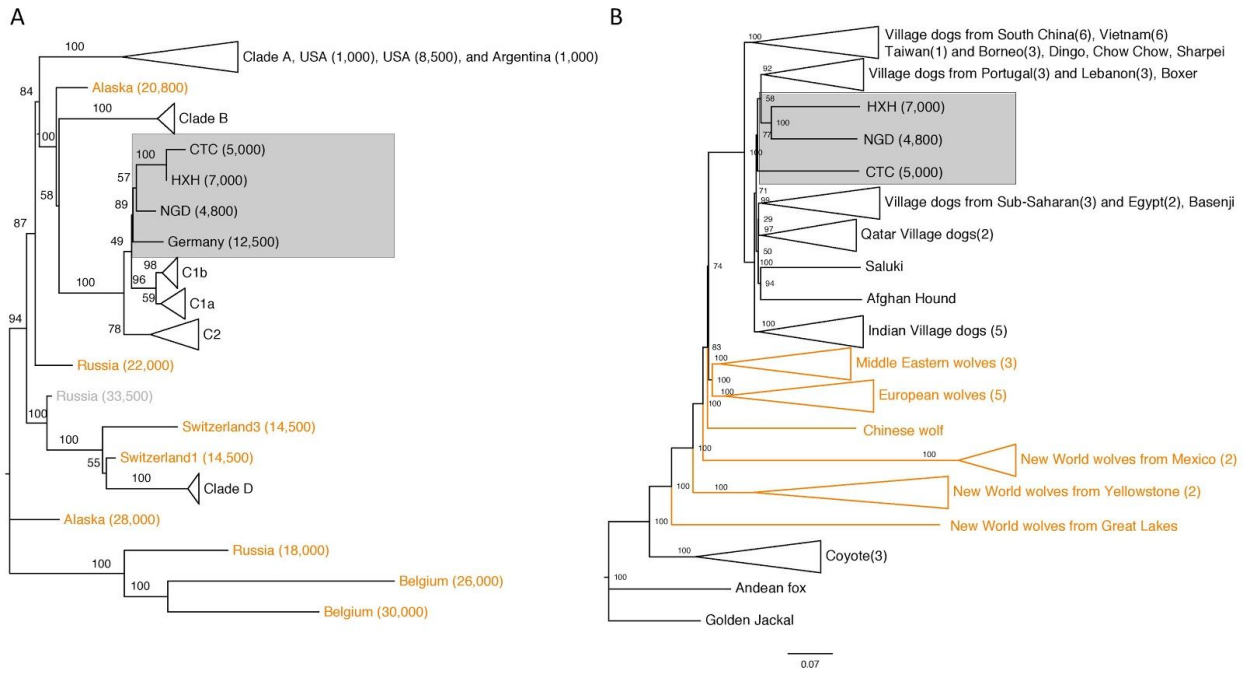

Figure 1. Phylogeny of ancient and contemporary canids. A). Phylogeny based on mtDNA. Age of the samples is indicated in parentheses, wolf samples shown in orange. **B)** Neighbor-joining tree based on pairwise sequence divergence from whole genome data.

Genomic clustering of the European Neolithic dogs

We constructed a neighbor-joining (NJ) tree using the whole genome dataset (Figure 1B) to determine which modern dog population shows the greatest genetic similarity with the ancient samples. We found that the Early Neolithic HXH and Late Neolithic NGD grouped together as a sister clade to modern European village dogs, while CTC was external to this clade, but still more similar to it than any other modern canid population. As shown previously (Frantz et al. 2016), East Asian village and breed dogs are basal to all other dogs.

We also performed a PCA using both the SNP array and whole genome data (Figure 2A, 2B and Supplementary Methods 8). The larger SNP array reference dataset shows that village dogs primarily separate into five geographically distinct clusters: Southeast Asia (Vietnam, Indonesia, Thailand, China), India, Middle East (Lebanon, Qatar, Turkey, Saudi Arabia, Armenia, Iraq), Europe, and Africa. Breed dogs fall mostly within European village dogs' variation with the exception of basal or "ancient" breeds (Larson et al. 2012), which are located within the axis of their geographical origin. Consistent with NJ tree analysis, all three ancient samples fell within the range of modern dog variation (we note that the position of NGD is radically different to that reported by Franz et al. (Frantz et al. 2016) (Supplementary Methods 15). HXH and NGD are the ancient samples found closest to the major European cluster, both lying adjacent to the cluster of Pacific Island dogs that are thought to be derived almost completely from European dogs (Shannon et al. 2015). CTC is located next to village dogs from Afghanistan, a known admixed population also inferred to have a major European-like ancestry component (Shannon et al. 2015).

We further examined the genetic relatedness between ancient and modern dogs by performing an $f3$-outgroup analysis on both the SNP array and whole genome datasets. This method has been used previously in ancient DNA studies to investigate how modern populations are genetically related to an ancient sample (Rasmussen et al. 2014; Allentoft et al. 2015; Jones et al. 2015; Hofmanová et al. 2016). Assuming a simple three population model with no post-divergence gene flow, where population C is an outgroup to A and B, the value of this statistic will reflect the amount of shared drift between A and B relative to C. We used the golden jackal and Andean fox as outgroups for the SNP array and the whole genome datasets, respectively. If one population (e.g. B) is kept constant, in this case an ancient dog, then introducing different populations to represent A will provide relative estimates of genetic

similarity with B. Results corroborated NJ tree and PCA findings, and showed that all three Neolithic European samples share most of their ancestry with modern dogs from Europe (Figure 3 and Supplementary Figures S10.1.1-2, Supplementary Methods 10).

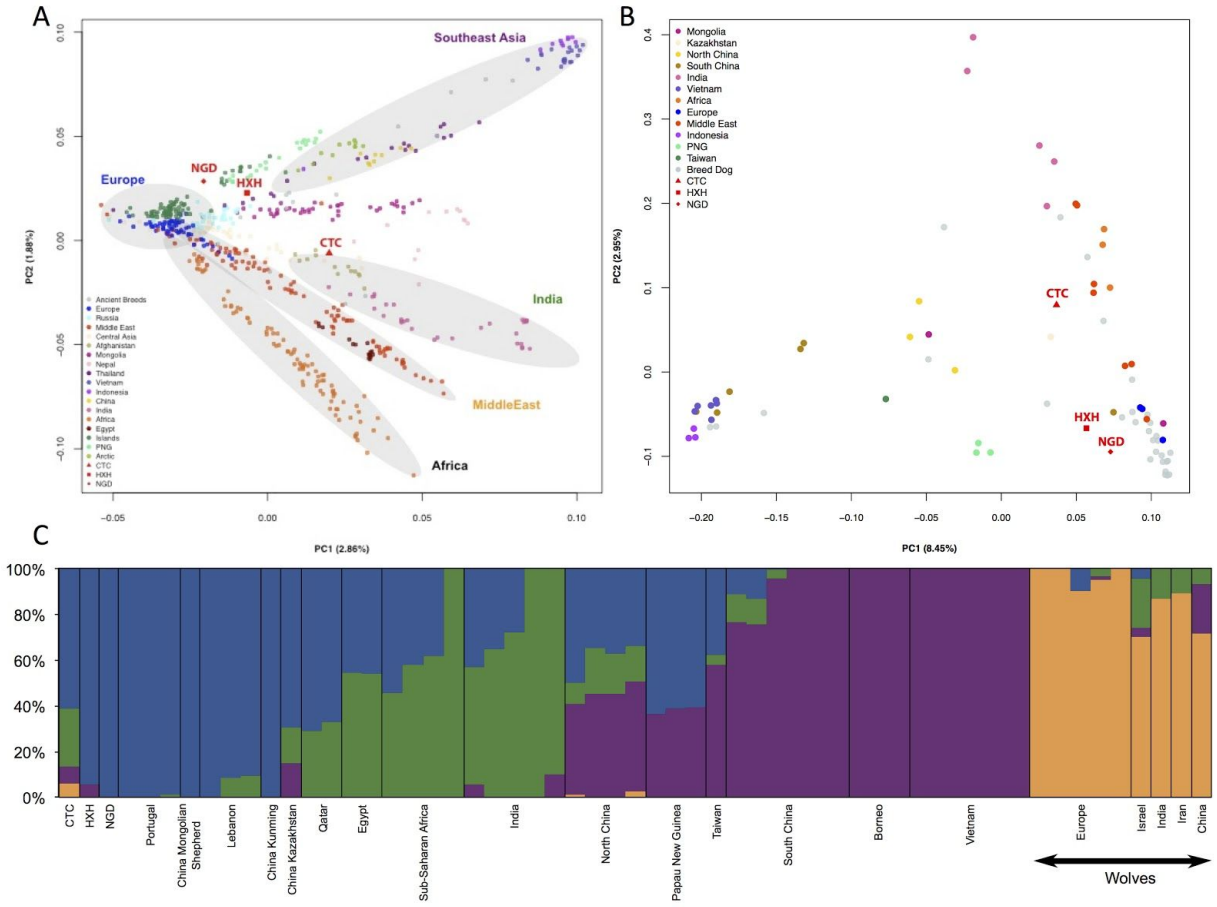

Figure 2. PCA and population structure between ancient and contemporary canids. A). PCA of village dogs, with breed dogs and ancient dogs projected onto the PC space using SNP array data. **B)**. PCA of village dogs, breed dogs and ancient dogs using whole genome SNP data ascertained in the New World wolves. **C)**. NGSadmix clustering for K=4 for village dogs, ancient dogs and Old World wolves based on the whole genome SNP data.

Evidence of admixture in Neolithic dogs

Our results are consistent with continuity of a European-like genetic ancestry from modern dogs through the entire Neolithic period, and, based on mtDNA from Bonn-Oberkassel, perhaps even into the Upper Paleolithic. However, the slightly displaced position of the ancient samples from the European cluster in the PCAs (particularly for CTC) suggests a complex history possibly involving ancestry from other sources. We therefore performed an unsupervised clustering

analyses with ADMIXTURE (SNP array data, Supplementary Figure S8.3.2) and NGSadmix (whole genome data, Figure 2C and Supplementary Figure S8.4.1) (Supplementary Methods 8) and found that, unlike contemporary European village dogs, all three ancient genomes possess a significant ancestry component that is present in modern Southeast Asian dogs (though to a lesser extent for NGD). This component appears only in a minority of modern European village dogs at very low levels. Furthermore, CTC harbors an additional component that is found predominantly in modern Indian village dogs as well as some wolf admixture.

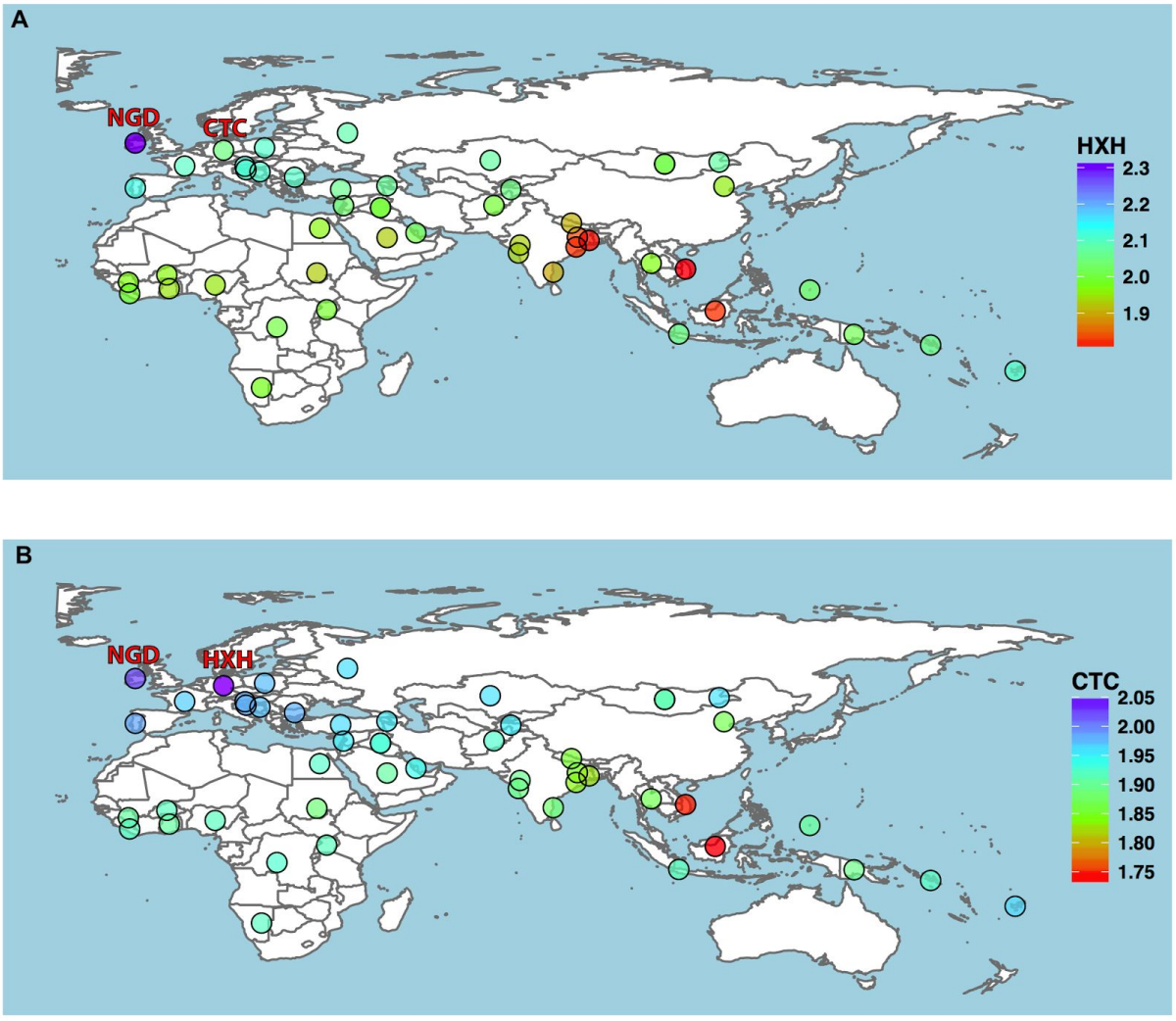

Figure 3. Genetic affinity of ancient samples. Heat map of outgroup *f3*-statistics of the form *f3* (golden jackal; ancient sample; X) based on SNP array genotype data. Higher *f3* values indicate increased shared drift between the samples, and therefore higher genetic similarities. **A)**. HXH shows greatest similarity with NGD and modern European village dogs (higher *f3* values), and is most distant to East Asian and Indian village dogs. **B)**. CTC shares the most genetic similarity with HXH, followed by NGD and other European dogs. In addition, CTC shows greater similarity to village dogs from India (particularly unadmixed populations in the east) than HXH does.

We formally modelled these potential admixture events by applying the tree-based framework, MixMapper (Lipson et al. 2013) to both the SNP array and whole genome data. This approach interrogates every pair of branches in a scaffold tree to infer putative sources of admixture for non-scaffold target samples (in this case HXH, CTC and NGD) via the fitting of *f-statistics* observed in the data. We constructed the scaffold tree excluding those populations that showed evidence of admixture as determined by an *f3* statistic test (see Supplementary Methods 10). MixMapper inferred that HXH and NGD were both formed by an admixture event involving the ancestors of modern European and Southeast Asian dogs. An *f4*-ratio test estimated ~15% and 8% Southeast Asian-like gene flow into HXH and NGD, respectively (Supplementary Methods 10). Analysis with ADMIXTUREGRAPH (Patterson et al. 2012), a method related to MixMapper that examines a manually defined demographic history, demonstrated a perfect fit for the observed *f-statistics* under this model (Supplementary Methods 11).

In order to disentangle the more complex admixture patterns observed in CTC, we first sought to understand its relationship with HXH given that both samples come from the same geographic region. Interestingly, we found an indication of possible genetic continuity between both samples with our *f3*-outgroup analysis, which revealed that CTC had greater affinity with HXH than with any modern canid or with NGD (Figure 3B, Supplementary Figure S10.1.1-2 and Supplementary Methods 10). We therefore performed a MixMapper analysis where HXH was set as one of the sources of admixture for CTC. This analysis gave far more interpretable results than a scenario that utilized solely contemporary populations in the scaffold, where multiple sometimes incompatible potential admixture events were identified for CTC involving branches leading to modern European, Indian, East Asian, Middle Eastern and wolf populations. Instead, when HXH was set as one of the sources of admixture, MixMapper identified a population ancestral to modern Indian village dogs as the second source of admixture for CTC, supporting the pattern identified in the unsupervised clustering analyses, and was quantified to contribute to around 19% of CTC's genome by an *f4*-ratio test.

However, given that HXH and modern European dogs share substantial genetic ancestry, it is possible that the observed European-like component in CTC is derived from a different lineage from HXH (for example, via a distinct European-Indian admixed population that migrated into Germany sometime during the Neolithic). Therefore, we used ADMIXTUREGRAPH to compare a model of canid demography where a) CTC descended from the same population as HXH

followed by admixture with an Indian-like population versus b) both ancient samples being descended from independently diverged European lineages. The model of CTC being a descendant of HXH (Figure 4A) provides a much better fit to the data. This scenario produced only two *f4* outliers (no *f2* or *f3* outliers), one of which was barely significant (Z=3.013), whereas a model where the two ancient samples are descended from different ancestral European populations produced 74 outliers (Supplementary Methods 11). Even though there is the risk of overfitting the model to the data, the stark difference in the fit of the two models point to general continuity amongst German dogs during the Neolithic, along with admixture towards the latter end of this era with an outside source similar to modern Indian village dogs.

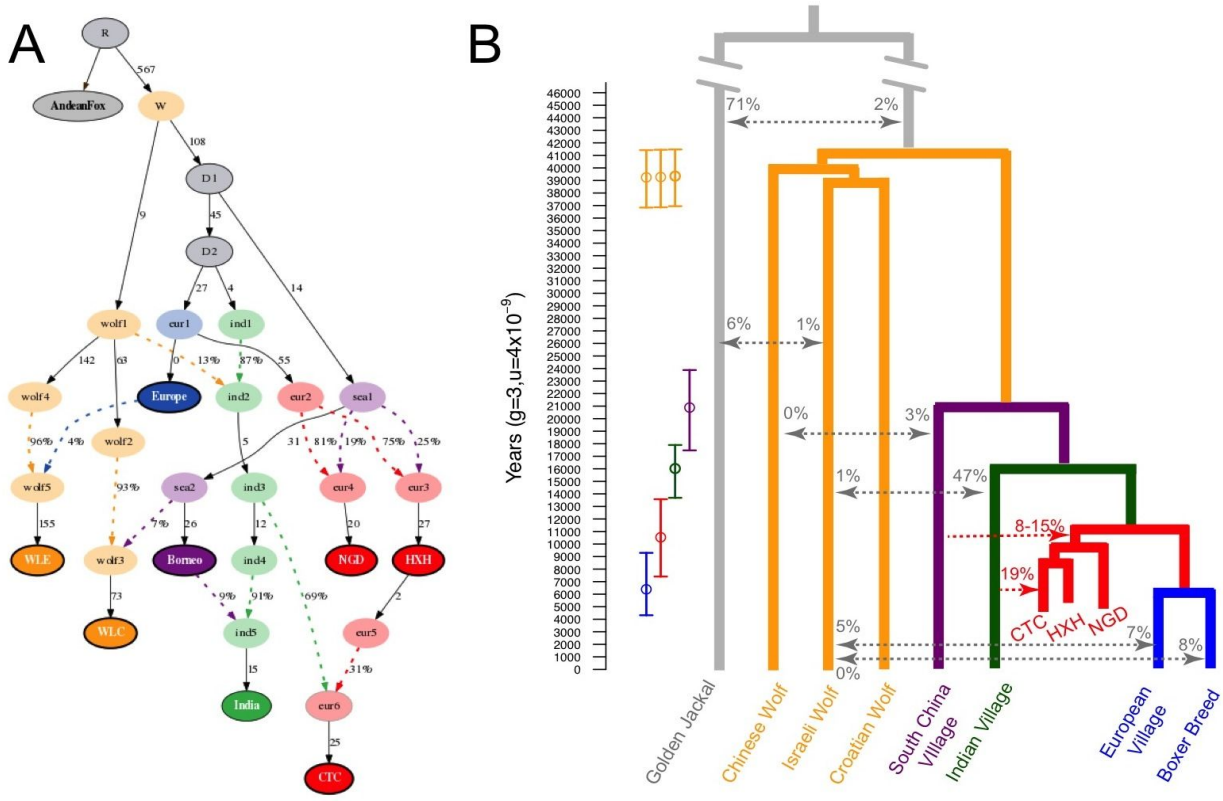

Figure 4. Demographic model regarding ancient and contemporary dogs and wolves. A). The best model fit to both modern and ancient canid data using ADMIXTUREGRAPH. This model had four *f4-statistic* outliers. Branches indicated by solid black lines (adjacent numbers indicate estimated drift values in units of *f2* distance, parts per thousand), admixture indicated by coloured dashed lines (adjacent numbers indicate ancestry proportions). Sampled individuals/populations indicated by solid circles with bold outline. **B).** Divergence times of contemporary dogs and wolves inferred using G-PhoCS. Mean estimates are indicated by circles with ranges correspond to 95% Bayesian credible intervals. Migration bands are shown in grey with associated value representing the inferred total migration rates (the probability that a lineage in the target population will migrate into the source population). The divergence time for HXH and NGD and modern European dogs is inferred using a numerical approach. The proportion of Indian village dog ancestry in CTC and South China village dog ancestry in HXH and NGD are inferred by *f4* ratio test, shown in red.

We further investigated the wolf admixture inferred by the unsupervised clustering analysis with SpaceMix (Bradburd et al. 2015), a method similar to PCA that additionally incorporates the geographic location of the populations to create a "geogenetic" map (Supplementary Methods 8). It then detects deviations of increased covariance in this geogenetic space that are likely to reflect long-distance admixture events. The clustering of modern and ancient dogs in SpaceMix is essentially the same as observed in the PCA, with HXH and NGD closest to Pacific Island dogs and CTC found near Afghanistan dogs. However, SpaceMix additionally inferred around 10% ancestry in CTC (but not HXH or NGD) from the geogenetic space containing Old World wolves (Supplementary Figure S8.2.3). *f4* statistics of the form *f4*(CTC,HXH,Wolf,Outgroup) suggest that the likely origin of this wolf component is related to contemporary Iranian/Indian wolves (those with the least amount of dog admixture, as revealed using an *f4*-ratio test and SpaceMix, Supplementary Methods 10). In light of these results, it is likely that a dog population carrying both Indian and wolf ancestry admixed with the population represented by CTC. We find support for this scenario with ADMIXTUREGRAPH, where a model for CTC incorporating modern village dogs and wolves produces no outliers when we allow for an admixture event between European and Indian village dog lineages along with previous wolf gene flow into the Indian lineage (Supplementary Methods 11, Supplementary Figure S11.2.1.).

This complex pattern of admixture found in CTC is similar to that observed in many modern dog populations in Central Asia (such as Afghanistan) and the Middle East, as shown in our unsupervised clustering analyses (Supplementary Figure S8.3.2). This raises the question of whether CTC and these modern dog populations share a common admixture history and are descended from the same ancestral populations. We performed a MixMapper analysis including HXH in the scaffold tree and observed that CTC draws its European-like component exclusively from this Early Neolithic German population (consistent with the ADMIXTUREGRAPH results). To the contrary, modern Afghanistan dogs generally demonstrate inferred ancestry from modern European village dogs. This suggests that modern Afghanistan village dogs and CTC are the result of independent admixture events, which in turn implies that dog gene flow across Eurasia has been occurring for thousands of years, illustrating the complex history of dog domestication.

Demographic model and divergence time

The distinct genetic makeup of the European Neolithic dogs from that of modern European dogs indicates that while ancient and contemporary populations share substantial genomic ancestry,

some degree of population structure was present in the continent. Neolithic dogs would thus represent a now extinct branch that is somewhat diverged from the modern European clade. In addition, our best fit model of modern and ancient canid demography using ADMIXTUREGRAPH involved a topology that would be consistent with a single dog lineage diverging from wolves (Figure 4A). Therefore, we attempted to infer the divergence time of HXH and NGD from modern European dogs after divergence of the Indian lineage, that according to the NJ tree analysis is the sister clade of the Western Eurasian branch (we note that this is a simplistic bifurcating model of what may have been more complex European geographic structuring).

We first used the coalescent-based G-PhoCS (Gronau et al. 2011) analysis of the model in Figure 4B to obtain estimates of divergence time and population diversity. Analysis was performed on sequence data from 16,434 previously identified 1kb-long loci (Freedman et al. 2014). Unlike the SNP-based analysis described above, single-sample genotype calling was performed with no particular ascertainment scheme, and as such we restricted our analysis to 8 medium to high coverage canid genomes, with coverage ranging from 8 to 24x. When we included only modern dogs, we observed that different modern wolf populations appeared to diverge rapidly, concordant with previous studies (Fan et al. 2016; Freedman et al. 2014), whereas the branching of the main dog lineages took place over a much longer period of time. We found that the (uncalibrated) dog-wolf divergence time in units of expected numbers of mutations (0.5247) was similar to that reported in Freedman (Freedman et al. 2014); however, our dog divergence time (0.2786) was younger than the Freedman et al. (Freedman et al. 2014) estimate but similar to the Wang et al. (Wang et al. 2016) estimate, most likely as a result of using Southeast Asian village dogs rather than the Dingo. We also found that the effective population size of village dogs was 5-10 fold higher than that of the Boxer.

However, when the ancient samples were included in the G-PhoCS analysis, all divergence times increased markedly (except the Boxer - European village dog split). Additionally, we detected an excess of private variants in the ancient samples (even for NGD, which was at high coverage) compared to European village dogs. It is thus likely that remnant post-mortem damage artificially inflated variation in the ancient samples and elongated the branch lengths in the G-PhoCS analysis. Therefore, we devised a new method for estimating the HXH-European split time, τ_1 (again, in units of expected numbers of mutations), that utilized G-PhoCS results for

only the modern samples and would be robust to biases resulting from the use of ancient samples (Supplementary Methods 13 and Supplementary Figure S13.2.1).

Specifically, we calculated the relative observed amount of derived allele sharing exclusive to European village dogs and HXH/NGD versus that exclusive to European and Indian village dogs. The two major advantages of this estimate are that a) it only depends on sites for which there is already evidence of a mutation in other higher coverage modern dogs (i.e. our genotype calling in ancient samples is likely to be much more accurate in such situations), and b) it uses only a single chromosome from each population (which can be randomly picked), and thus does not require calling heterozygotes accurately (i.e. it should not be sensitive to the lower coverage of our ancient samples). We then calculated the expectation of this ratio using coalescent theory (see Methods) and iterated over possible τ_1 values until the expectation of the ratio fell into the observed confidence interval (as expected considering the tree topology, European dogs share more derived alleles with the ancient dogs than Indian village dogs, with ratios of 1.186-1.217 for HXH and 1.195-1.231 for NGD). Our expectation was conditioned on the following parameter estimates from G-PhoCs: N_e for European/Boxer ancestral population (θ_1), N_e for European/Indian ancestral population (θ_2), time of divergence for Europe and Boxer (τ_0), time of divergence for Europe/India (τ_2) and time of divergence for Europe-India/Asia (τ_3), as well as the percentage of HXH that is made up of Asian admixture (α) from the *f4*-ratio analysis.

While our estimates of divergence times are in units of expected numbers of mutations, we can use the age of our ancient samples to calibrate the resulting divergence time in years. Specifically, we used the age of the HXH sample to set an upper bound to the yearly mutation rate μ, as the sample must be younger than the time in years since divergence of HXH and modern European dogs. Given that the sample is 7,000 years old, μ has an upper bound with mean value 6.0×10^{-9} per generation (assuming a 3 year generation time) and 95% CI of 4.23×10^{-9} to 7.8×10^{-9} (Supplementary Figure S13.5.1.c), which is consistent with the $\mu = 4 \times 10^{-9}$ per generation suggested by Skoglund et al. (Skoglund et al. 2015) (0.4×10^{-8} per base per generation, 3 years per generation). When we calibrate τ_1 using this mutation rate, we estimate a value of ~7,400-13,500 years for HXH and ~8,400-13,600 years for NGD. From the G-PhoCS analysis, we further estimated that modern European and Indian village dogs diverged ~13,700-17,900 years ago, both of which diverged from Southeast Asian dogs ~17,500-23,900

years ago as a basal dog divergence event. We also estimated the dog-wolf divergence time to be 36,900-41,500 years ago (Figure 4B).

Functional variants associated with the domestication process

As a result of domestication from wolves, portions of dog genomes have significantly differentiated from their wild counterparts (Axelsson et al. 2013). To determine the domestication status of the three Neolithic dogs, we assessed haplotype diversity at eighteen candidate domestication loci originally identified using breed dogs and wolf populations (Axelsson et al. 2013) (Supplementary Methods 14) which showed patterns consistent with selection across our panel of village dogs. HXH appeared homozygous for the dog-like haplotype at all but one locus, and thus was often indistinguishable from most modern dogs. The younger NGD appeared dog-like at all but two loci. CTC, however, was heterozygous for the wolf-like haplotype at six loci, compatible with its increased wolf ancestry described above (Supplementary Figure S8.2.3. and Supplementary Methods 8).

The Neolithic saw drastic changes in human culture and behavior, including the advent of agriculture, resulting in a shift toward more starch-rich diets. Elevated *AMY2B* copy-number, which is associated with increased starch metabolism efficiency, has traditionally been suggested to be a strong candidate feature of domestication, even though *AMY2B* copy-number is known to vary widely in diverse collections of modern wolves and breed dogs (Arendt et al. 2014; Reiter et al. 2016; Freedman et al. 2014). Although the dog haplotype is present in all three Neolithic samples (Figure 5A), none showed evidence for the extreme copy number expansion of *AMY2B* (Figure 5B). Based on read depth, we estimate that CTC and HXH carried two copies of the *AMY2B* gene while NGD carried three copies (Supplementary Methods 14). Analysis of the full sample set of canines shows a bimodal distribution of copy number, with most dogs having >6 *AMY2B* copies, while few carry 2 or 3 copies (Reiter et al. 2016). This dynamic and extreme copy-number increase is presumed to be the result of a tandem expansion of the AMY2B gene (Axelsson et al. 2013). Further analysis of NGD read-depth profiles reveals the presence of a larger, ~2 megabase segmental duplication encompassing the *AMY2B* gene locus on chromosome 6 and extending proximally toward the centromere. This duplication is present in eleven of the analyzed samples and appears to be independent of the extreme copy number expansion of the *AMY2B* gene itself (Supplementary Methods 14).

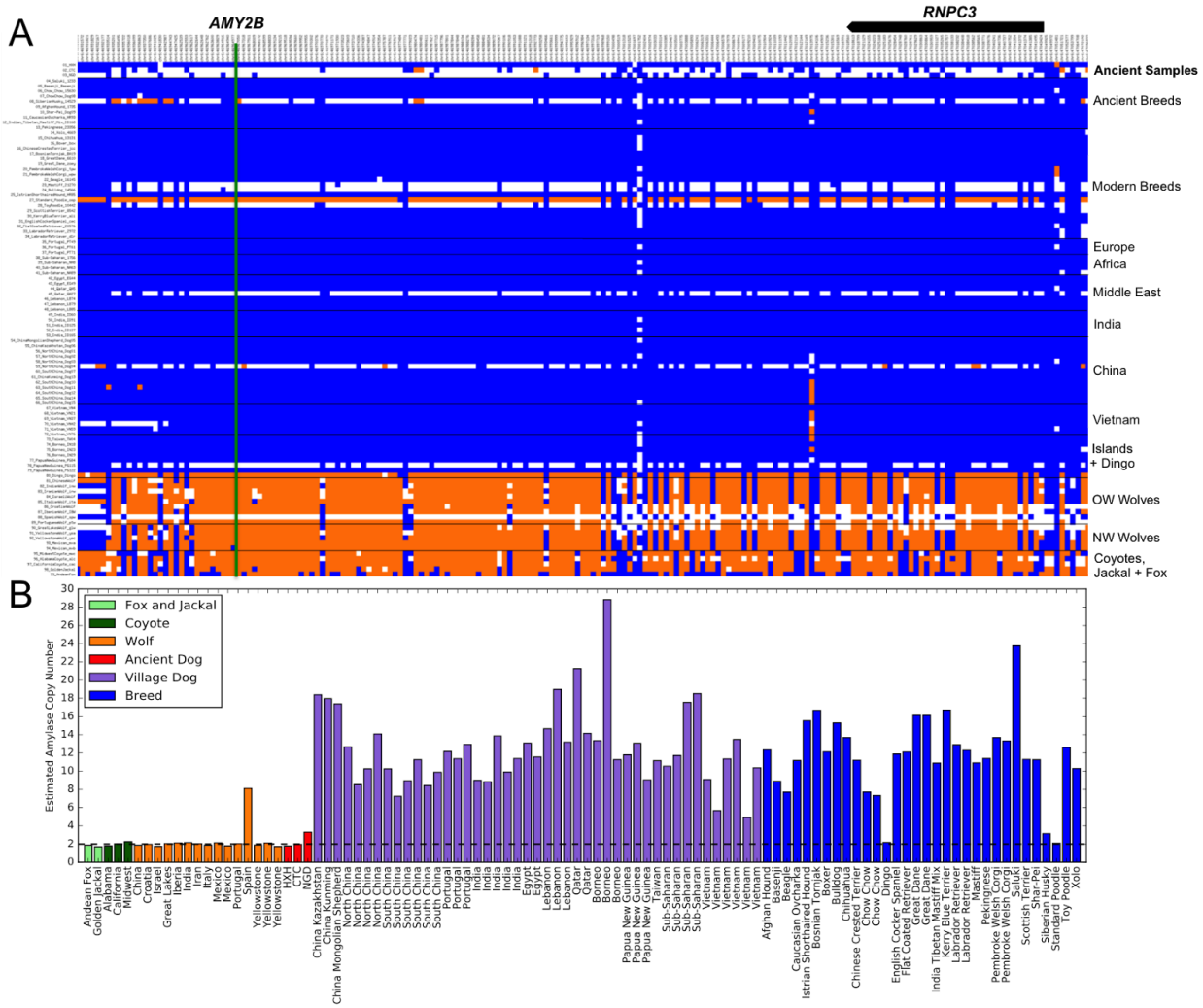

Figure 5. Haplotype and copy-number variation at the amylase 2B (*AMY2B*) locus. A). Genotype matrix of selected sites within F_{ST}-derived domestication locus 12 (chr6: 46854109-47454177)(Axelsson et al. 2013). SNP genotypes are represented as either homozygous for the reference allele (0/0; blue), heterozygous (0/1; white), or homozygous (1/1; orange) for the alternate allele. The positions of *AMY2B* (green line) and *RNPC3* (model above) are indicated. **B)**. Read-depth based estimation of *AMY2B* copy number for the Andean fox (light green), golden jackal (light green), coyotes (dark green), wolves (orange), ancient samples (red), village dogs (purple), and breed dogs (blue). Dashed line indicates diploid copy number of two.

Discussion

The direct analysis of two Neolithic samples from Central Europe provides a number of new insights in the history of dog domestication. We do not find evidence of a remnant European Paleolithic dog population contributing solely to the genetic architecture of ancient dogs from either the Early or End Neolithic and therefore our results do not support the hypothesis of a

population replacement during the Neolithic. Instead, we find that NGD is genetically very similar to HXH, both with ~75-80% of modern European-like ancestry as estimated with MixMapper or ADMIXTUREGRAPH. Additionally, CTC is most likely descended from a population represented by HXH, pointing to some genetic continuity throughout the Neolithic in that region. We find further support for this genetic continuity in the mtDNA phylogeny, which places all the ancient samples, including an Upper Paleolithic 12,500 years old German dog, together within sub-haplogroup C1 and as a sister clade of C1a and C1b.

However, the admixture events observed in European Neolithic dogs but not in modern dogs from the same region suggest some degree of population structure in the continent during that period. This is further supported by HXH and NGD carrying Southeast Asian ancestry but lacking ancestry shared between modern Indian village dogs and CTC, even though NGD and CTC are almost contemporaneous (4,800 vs. 4,700 years old). It is likely that a different subpopulation from a structured European Neolithic population eventually became dominant in modern European dogs, which may have also provided an opportunity for the observed mtDNA turnover from haplogroup C to A, especially if this subpopulation also passed through a strong bottleneck or mtDNA was also structured in the continent. The clustering of the ancient samples within C1 into a different sub-haplogroup than modern dogs also points to some degree of substructure.

The age of the samples provide a time frame, between ~7,000 and 5,000 years ago, for CTC to obtain its additional Indian-like ancestry component. Considering that CTC shows similar admixture patterns to Central Asian and Middle Eastern modern dog populations, as seen in the PCA (Figure 2) and ADMIXTURE (Supplementary Figure S8.3.2.) analysis, and that the cranium was found next to two individuals associated with the Neolithic Corded Ware Culture, we speculate that the Indian-like gene flow may have been acquired by admixture with incoming populations of dogs that accompanied steppe people migrating from the East. Moreover, ADMIXTUREGRAPH and *f4* statistics support the possibility that the Indian and the wolf ancestry are the consequence of the same admixture event, involving a dog population that carried the two ancestries. This scenario is further supported by the model estimated by G-PhoCS, which infers substantial migration from wolves to the lineage represented by Indian village dogs (and as much as 0.36 migration rate when Indian wolves are included in the tree (Supplementary Methods 12)).

Using a mutation rate of $4x10^{-9}$ we estimate that the population ancestral to European and Indian lineages diverged from Southeast Asian dogs around ~17,500-23,900 years ago. This "east-west" divergence time is compatible with that reported by Wang et al. (Wang et al. 2016), but is considerably older than the one recently reported by Frantz et al. (Frantz et al. 2016). We note that when we used the mutation rate from Freedman et al. (Freedman et al. 2014) to calibrate our divergence time (1×10^{-8} per generation, generation time 3 years), we obtained a value in years that was incompatible with the age of the sample (estimated divergence time of ~4,000 years compared to ^{14}C age of ~7,000 years). Given our older estimate of divergence time between Southeast Asian and European dog populations compared to Frantz et al. (Frantz et al. 2016) (see Supplementary Methods 15) and our best model of population demography (Figure 4), our results can most parsimoniously be explained by a single domestication process for dogs. If there was a replacement of a highly distinct European dog lineage with independent domestication origins to that of dogs in Asia, it must have occurred prior to the Neolithic (and perhaps much earlier given the matrilineal continuity between HXH, CTC and Bonn-Oberkassel). However, currently we find no genetic evidence that supports the recently proposed hypothesis of a dual domestication processes for dogs. Clearly, analysis of additional spatiotemporally diverse ancient genomes is required to better understand the possibly complex admixture processes that occurred during this period, while older specimens, particularly from Asia, will be necessary to resolve the history of dog domestication.

We also estimated the dog-wolf divergence time to be 36,900-41,500 years (Figure 4B), which is consistent with predictions from the ancient Taimyr wolf genome (Skoglund et al. 2015). Domestication must have occurred subsequent to the dog-wolf divergence and prior to Southeast Asian divergence, and therefore our results provide an upper and lower bound for the start of dog domestication, which would be between ~20,000 and 40,000 years ago. However, whether this reflects a much older start of the dog domestication process than predicted by archaeological material (such as Bonn-Oberkassel) or a more recent descent of dogs from thus far unknown wolf populations remains an open question.

Arising from numerous tandem duplication events, enhanced starch digestion through extreme *AMY2B* copy number expansion has been postulated to be an adaptation to the shift from the carnivorous diet of wolves to the starch-rich diet of domesticated dogs (Axelsson et al. 2013).

Although none of the German Neolithic samples carries the copy-number expansion of the *AMY2B* gene associated with starch digestion, we find that this gene is present in three copies in NGD. The increased copy number in the Irish NGD sample is due to a large segmental duplication that is shared with multiple modern dogs, an event separate from the tandem *AMY2B* duplications. This suggests that the initial selection at this locus may have been independently driven by some factor other than *AMY2B* copy number. Furthermore, the absence of the extreme *AMY2B* copy number increase in these ancient samples indicates that the selective sweep associated with *AMY2B* expansion must have occurred after the advent of agriculture and the Neolithic. This is consistent with recent findings that *AMY2B* copy number is bimodal, highest in modern dog populations originating from geographic regions with prehistoric agrarian societies, and lowest from regions where humans did not rely on agriculture for sustenance (Arendt et al. 2016). The absence of *AMY2B* expansion in dogs from non-agrarian regions (i.e. Arctic breeds and the Australian dingo) supports the claim that the expansion occurred after the initial domestication, and possibly after the migration of dingoes to Australia (3,500-5,000 years ago) (Arendt et al. 2016). A similar delayed pattern has been observed in humans, where alleles associated with lactase persistence in Europe rose to significant frequencies during the Bronze Age, i.e. 3,000 years after the introduction of milkable livestock (Allentoft et al. 2015).

Overall, the analysis of two Neolithic samples from Central Europe from nearby regions has revealed an intricate history of dog domestication. While we find solid evidence of overall genetic continuity throughout the Neolithic and up to the present, our results also reveal genetic structure at least within the European continent and more importantly substantial gene flow from different sources from Asia. Our results show that these admixture events are different from the ones we observe in modern dog populations, and therefore suggest that, as has been recently shown for humans (Haak et al. 2015; Allentoft et al. 2015; Hofmanová et al. 2016), dog population movements have been somewhat common throughout history. The inference of complex patterns of gene flow remains challenging when only modern samples are studied. Therefore, the acquisition of a larger sample set including ancient representatives from the Middle East, Central and Southeast Asia will be crucial to clarify the details of dog domestication and diversification throughout the world.

Methods

Archaeological Background

HXH. A single petrous bone was identified in the internal ditch structure of Herxheim, an Early Neolithic site in Germany discovered in 1996 containing archaeological material from the Linearbandkeramik culture. Herxheim contains a significant amount of faunal remains, including >250 remains from dogs that constitute the largest bone series of Early Neolithic dogs in western Europe. A ^{14}C dating of 5223-5040 cal. BCE (95.4 %) was estimated for the bone (Mams-25941: 6186+/-30, calibrated with OxCal 4.2 (Ramsey 2009) using the IntCal13 calibration curve (Reimer et al. 2013)).

CTC. The entire cranium of a dog was found in the Kirschbaumhöhle (Cherry Tree Cave) in the Franconian Alb, Germany (Seregély et al. 2015). The cave was discovered in 2010 and contains human and animal remains from at least six prehistoric periods. CTC was an adult dog demonstrating morphological similarity to the so-called Torfhund (*Canis familiaris palustris*), and was found close to two human skulls dated to the early End Neolithic (2,800 - 2,600 cal. BCE). A ^{14}C dating of 2,900-2,632 cal. BCE (95.4 %) was estimated for the cranium (Erl-18378: 4194+/-45, calibrated with OxCal 4.2 using the IntCal13 calibration curve). See Supplementary Methods 1 for more details.

DNA Isolation and Screening

HXH. The petrous part of the temporal bone of sample HXH was prepared in clean-room facilities dedicated to ancient DNA in Trinity College Dublin (Ireland). DNA extraction was performed using a Silica column method as described in MacHugh et al. (MacHugh et al. 2000). Two genomic libraries were prepared as described in Gamba et al. (Gamba et al. 2014). Screening of one library via an Illumina MiSeq run and mapping against various reference genomes demonstrated that reads for this sample mapped almost exclusively to the CanFam3 genome, revealing that it was a canid. Blank controls were utilized throughout. See Supplementary Methods 2 for more details.

CTC. Sample preparation was conducted in dedicated ancient DNA facilities of the Palaeogenetics Group at Johannes Gutenberg-University Mainz under strict rules for contamination prevention as described in Bramanti et al. (Bramanti et al. 2009). DNA was extracted independently twice from the petrous bone using a phenol-chloroform protocol (Scheu

et al. 2015). A total of four double indexed genomic libraries were prepared as described in Hofmanová et al. (Hofmanová et al. 2016). One library was screened for endogenous DNA content via Illumina MiSeq sequencing, with 61.5% of reads mapping to CanFam3. Blank controls were utilized throughout. See Supplementary Methods 3 for more details.

Genome sequencing and Bioinformatic Processing

Combinations of various genomic libraries from each ancient sample (CTC and HXH) were sequenced on two lanes of an Illumina HiSeq 2500 1TB at the New York Genome Center (NYGC) using the High Output Run mode to produce 2x125 bp paired-end reads. Reads were trimmed, merged and filtered using a modified version of the ancient DNA protocol described by Kircher (Kircher 2012). Merged reads were then mapped using `BWA aln (Li and Durbin 2010)` to a modified version of the CanFam3.1 reference genome containing a Y chromosome. Duplicate reads were identified and marked using `PICARD MarkDuplicates`, resulting in a mean coverage for both samples of 9x. Additionally, the mean coverage for the X and Y chromosomes was ~5x for both samples, indicating they were males. Mean fragment length for both samples ranged from 60-70bp. Post-mortem degradation effects were assessed using `MapDamage_v1.0 (Ginolhac et al. 2011)`, revealing extensive 5' C>T and 3' G>A damage. Single-ended reads for the NGD extracted from a `BAM` file containing all mapped reads were processed using the same pipeline. See Supplementary Methods 4 for more details.

Genotype likelihood estimation and genotype calling for all three ancient samples was performed using a custom caller that takes into account post-mortem damage patterns identified by `MapDamage` based on the model described in Hofmanová et al. (Hofmanová et al. 2016). Briefly, damage patterns with respect to read position are fit with a Weibull distribution of the form a X exp(-(x^c) X b), where x is the proportion of damaged C>T or G>A bases at a particular position along the read (unlike Hofmanová et al. (Hofmanová et al. 2016), we find a slightly better fit with a Weibull than when assuming exponential decay, Supplementary Figure S5.1.1). Any site with less than 7x coverage was reported as missing. In addition, any position where the highest likelihood is a heterozygote must have a minimum Phred-scaled genotype quality of 30 or the next highest homozygote likelihood genotype was chosen instead. The code is available at https://github.com/kveeramah/aDNA_GenoCaller. This protocol substantially decreased the overrepresentation of C>T and G>A sites identified by `GATK UnifiedGenotyper (DePristo et al. 2011)`, which does not account for post-mortem

damage. See Supplementary Methods 5 for more details. Additionally, base calls with a quality score less than 15 and reads with a mapping quality less than 15 were not included during genotype calling. Base calls with a quality score greater than 40 (which can occur during paired-end read merging) were adjusted to 40.

Reference Dataset

Genome Sequence Data. In addition to the three ancient samples, we examined whole genome sequence data from 96 modern canids. Additional genomes were generated using Illumina sequencing for a Great Dane and Iberian wolf. We also posted sequencing reads to the SRA for a Portuguese village dog, Chinese Mongolian Shepherd village dog and Afghan Hound. All remaining genome data were acquired from previously published datasets deposited on SRA. As above, reads for all modern canids were aligned to CanFam3.1 using `BWA`, followed by GATK quality score recalibration, and genotype calling using `HaplotypeCaller (DePristo et al. 2011)`. These data were supplemented with genotype data for six canids from Freedman et al. (Freedman et al. 2014) (Basenji, Dingo, golden jackal, Croatian wolf, Israeli wolf, and Chinese wolf). We generated three different call sets with different ascertainment schemes. Call set 1 includes all variants from both ancient and contemporary genomes, representing the most comprehensive set of variants, but may show biases due to differences in coverage among sample sets. Call set 2 only includes variants discovered in the three ancient genomes. Call set 3 only includes sites discovered as variable in New World wolves, and is the primary call set utilized for most analyses. See Supplementary Methods 6 for more details.

SNP array data. Canine SNP array datasets were obtained from Shannon et al. (Shannon et al. 2015) and Pilot et al. (Pilot et al. 2015). Genotypes were also supplemented by data from the six canids reported in Freedman et al. (Freedman et al. 2014).

Statistical Analysis

mtDNA. The average sequencing depth for mtDNA was 179x, 208x and 170x in the CTC, HXH and NGD samples, respectively. Ancient sample mtDNA consensus sequences were aligned to the canid alignment from Thalmann et al. (Thalmann et al. 2013), which contain whole mtDNA genomes for both modern and ancient canids. A NJ tree was built with a TN93 substitution model (500 bootstraps) using `MEGA 6.06 (Tamura et al. 2013)`. A further NJ tree was

built with additional C1 and C2 samples from Duleba et al. (Duleba et al. 2015). See Supplementary Methods 7 for more details.

Population Structure. Principle component analysis was performed on both the SNP array data set and genome SNP Call set 3 using `smartpca`, part of the `EIGENSOFT` package version 3.0 (Patterson et al. 2006). Both diploid and pseudo-haploid genotype calls with and without C<>T and G<>A SNPs (the most likely sites to undergo post-mortem damage) were used to construct the PCA, but little difference was found amongst these analyses. `SpaceMix (Bradburd et al. 2015)` was used to create a geogenetic map and infer potential long-distance admixture events across this map using the SNP array data, allowing only SNPs separated by at least 100kb and no more than five individuals per population. Multiple runs were performed with 10 initial burn-ins of 100,000 generations and a final long run of 10,000,000 generations. `ADMIXTURE` (v. 1.22) (Alexander et al. 2009) was used to perform an unsupervised clustering analysis on the SNP array data for the ancient dogs and a subset of 105 modern dogs that provided a global representation of dog structure, while `NGSadmix (Skotte et al. 2013)` was used to perform a similar analysis for the genome SNP data while taking into account genotype uncertainty by examining genotype likelihoods. Cross validation was performed for the `ADMIXTURE` analysis to identify the most appropriate number of clusters, *K*. See Supplementary Methods 8 for more details.

Neighbor-Joining tree construction. NJ trees were constructed for the whole genome SNP set using the `ape` R package (Paradis et al. 2004) using distance matrices based on the metric of sequence divergence from Gronau et al. (Gronau et al. 2011). One hundred bootstrap replicates were generated by dividing the genome into 5 cM windows and sampling with replacement in order to determine node support. See Supplementary Methods 9 for more details.

F and D-statistics-based analysis. Outgroup-*f3* statistics to assess relative genetic drift between ancient and modern dogs, *D*-statistics to identify potential ancient dog-wolf admixture and *f4*-ratio tests to estimate dog-dog and dog-wolf admixture proportions were calculated using `Admixtools (Patterson et al. 2012)`. Both `MixMapper (Lipson et al. 2013)` and `ADMIXTUREGRAPH (Patterson et al. 2012)` were used to perform model-based inference of specific admixture events involving the three ancient dogs for both the SNP array and whole genome SNP datasets. Significance was assessed using a weighted block jackknife

procedure for all five analysis types. Genetic map positions for each SNP used in these analyses were inferred from Auton et al. (Auton et al. 2013). See Supplementary Methods 11 and 12 for more details.

G-PhoCS and HXH divergence estimation. `G-PhoCS (Gronau et al. 2011)` was used to estimate divergence times, effective population sizes and migration rates for various modern dog and wolf combinations using sequence alignments from 16,434 "neutral" loci previously identified in Freedman et al. (Freedman et al. 2014) after `LiftOver` from CanFam3 to CanFam3.1. NJ trees were constructed to inform the topology of population divergence. 500,000 MCMC iterations were found to be sufficient for convergence for our data, with the last 200,000 used to estimate posterior distributions. We then developed a numerical approach based on coalescent theory to predict the ratio of shared derived sites between HXH/NGD and European village dogs versus Indian and European village dogs given the parameters estimated by `G-PhoCS` for European, Indian and Southeast Asian population divergence and a particular divergence time of HXH/NGD in units of expected numbers of mutations. Confidence intervals were estimated by resampling `G-PhoCS` parameters from their posterior distributions and finding predicted derived allele sharing ratios that were within a range determined for the observed data by a weighted jackknife resampling approach. See Supplementary Methods 11 and 12 for more details.

Genotyping at loci associated with the domestication process. Coordinates of thirty putative "domestication loci" were obtained from Axelsson et al. (Axelsson et al. 2013) and lifted over from CanFam2.0 to CanFam3.1 coordinates. Call set 1 SNPs within each window were extracted from the ancient samples and our genome sequence dataset. Eigenstrat genotype file formats were generated per window using `convertf` from the `EIGENSOFT` package (Price et al. 2006) and custom scripts were used to convert the genotype files into matrix formats for visualization using `matrix2png (Pavlidis and Noble 20 03)` using a filtered subset of SNPs (minor allele frequencies between 0.05 and 0.49) for easing visualization of the matrices. NJ trees were estimated for each window with the full SNP set using the same methods as the whole genome tree estimation (see above). Altogether, the haplotypes of the three ancient samples were classified as either dog or wolf-like for 18 matrices that showed clear distinction between dog and wild canid haplotypes based on average reference allele counts calculated per window. See Supplementary Methods 14 for more details.

Copy-number variation at the amylase 2B locus. Genomic copy-number was estimated from read depth as previously described (Sudmant et al. 2010; Alkan et al. 2009). Reads were split into non-overlapping 36-bp fragments and mapped to a repeat-masked version of the CanFam3.1 reference using `mrsFAST (Hach et al. 2010)`, returning all read placements with two or fewer substitutions. Raw read depths were tabulated at each position and a loess correction for local GC content was calculated utilizing control regions not previously identified as copy number variable. The mean depth in 3kb windows was then calculated and converted to estimated copy-number based on the depth in the autosomal control regions. See Supplementary Methods 14 for more details.

Data Access

Sequencing data is available from the NCBI sequence read archive (SRA) database under accession numbers SRS1407451 (CTC) and SRS1407453 (HXH), and mitochondrial genomes are available in GenBank under accessions KX379528 and KX379529, respectively.
Code generated to call variants in the ancient samples is available at:
https://github.com/kveeramah/aDNA_GenoCaller

Acknowledgements

We thank Dan Bradley for his help obtaining the HXH specimen. We thank Walter Eanes and Douglas Futuyma for their comments on the manuscript. We thank Dorina Twigg for the processing of canine copy-number variation data, Nick Patterson for providing advanced access to the latest version of `Admixtools`, Vida for his thoughts, the NYGC for their assistance in the sequencing, Valeria Mattiangeli for performing initial Miseq sequencing on HXH, and Christian Sell for his assistance with the raw data analysis pipeline used for the CTC Miseq data. The Kidd Lab is supported by grant R01GM103961 and Amanda Pendleton is supported by T32HG00040. Amelie Scheu and Kevin Daly are supported by the EU: CodeX Project No: 295729. Laura Botigué is supported by the Beatriu de Pinós Fellowship, from Generalitat de Catalunya. Shyamalika Gopalan was supported by a Boehringer Ingelheim Fonds Travel award.

Author contributions

T.S, A.Z and R.A provided the archaeological material. A.S, S.G, K.D and M.U performed the ancient DNA lab work and screening. L.R.B, S.S, A.L.P, M.O, A.M.T, D.B, J.M.K and K.R.V

performed the downstream bioinformatics and population genetic analysis. L.R.B, J.B and K.R.V conceived the study. L.R.B and K.R.V wrote the paper.

Disclosure Declaration

All authors declare no financial interests

References

Alexander DH, Novembre J, Lange K. 2009. Fast model-based estimation of ancestry in unrelated individuals. *Genome Res* **19**: 1655–1664.

Alkan C, Kidd JM, Marques-Bonet T, Aksay G, Antonacci F, Hormozdiari F, Kitzman JO, Baker C, Malig M, Mutlu O, et al. 2009. Personalized copy number and segmental duplication maps using next-generation sequencing. *Nat Genet* **41**: 1061–1067.

Allentoft ME, Sikora M, Sjögren K-G, Rasmussen S, Rasmussen M, Stenderup J, Damgaard PB, Schroeder H, Ahlström T, Vinner L, et al. 2015. Population genomics of Bronze Age Eurasia. *Nature* **522**: 167–172.

Anderson TM, vonHoldt BM, Candille SI, Musiani M, Greco C, Stahler DR, Smith DW, Padhukasahasram B, Randi E, Leonard JA, et al. 2009. Molecular and evolutionary history of melanism in North American gray wolves. *Science* **323**: 1339–1343.

Arendt M, Cairns KM, Ballard JWO, Savolainen P, Axelsson E. 2016. Diet adaptation in dog reflects spread of prehistoric agriculture. *Heredity* . http://dx.doi.org/10.1038/hdy.2016.48.

Arendt M, Fall T, Lindblad-Toh K, Axelsson E. 2014. Amylase activity is associated with AMY2B copy numbers in dog: implications for dog domestication, diet and diabetes. *Anim Genet* **45**: 716–722.

Auton A, Rui Li Y, Kidd J, Oliveira K, Nadel J, Holloway JK, Hayward JJ, Cohen PE, Greally JM, Wang J, et al. 2013. Genetic recombination is targeted towards gene promoter regions in dogs. *PLoS Genet* **9**: e1003984.

Axelsson E, Ratnakumar A, Arendt M-L, Maqbool K, Webster MT, Perloski M, Liberg O, Arnemo JM, Hedhammar A, Lindblad-Toh K. 2013. The genomic signature of dog domestication reveals adaptation to a starch-rich diet. *Nature* **495**: 360–364.

Benecke N. 1987. Studies on early dog remains from Northern Europe. *J Archaeol Sci* **14**: 31–49.

Bradburd G, Ralph PL, Coop G. 2015. *A Spatial Framework for Understanding Population Structure and Admixture*. http://biorxiv.org/lookup/doi/10.1101/013474.

Bramanti B, Thomas MG, Haak W, Unterlaender M, Jores P, Tambets K, Antanaitis-Jacobs I,

Haidle MN, Jankauskas R, Kind C-J, et al. 2009. Genetic discontinuity between local hunter-gatherers and central Europe's first farmers. *Science* **326**: 137–140.

Briggs AW, Stenzel U, Johnson PLF, Green RE, Kelso J, Prüfer K, Meyer M, Krause J, Ronan MT, Lachmann M, et al. 2007. Patterns of damage in genomic DNA sequences from a Neandertal. *Proc Natl Acad Sci U S A* **104**: 14616–14621.

Deguilloux MF, Moquel J, Pemonge MH, Colombeau G. 2009. Ancient DNA supports lineage replacement in European dog gene pool: insight into Neolithic southeast France. *J Archaeol Sci* **36**: 513–519.

DePristo MA, Banks E, Poplin R, Garimella KV, Maguire JR, Hartl C, Philippakis AA, del Angel G, Rivas MA, Hanna M, et al. 2011. A framework for variation discovery and genotyping using next-generation DNA sequencing data. *Nat Genet* **43**: 491–498.

Duleba A, Skonieczna K, Bogdanowicz W, Malyarchuk B, Grzybowski T. 2015. Complete mitochondrial genome database and standardized classification system for Canis lupus familiaris. *Forensic Sci Int Genet* **19**: 123–129.

Fan Z, Silva P, Gronau I, Wang S, Armero AS, Schweizer RM, Ramirez O, Pollinger J, Galaverni M, Ortega Del-Vecchyo D, et al. 2016. Worldwide patterns of genomic variation and admixture in gray wolves. *Genome Res* **26**: 163–173.

Frantz LAF, Mullin VE, Pionnier-Capitan M, Lebrasseur O, Ollivier M, Perri A, Linderholm A, Mattiangeli V, Teasdale MD, Dimopoulos EA, et al. 2016. Genomic and archaeological evidence suggest a dual origin of domestic dogs. *Science* **352**: 1228–1231.

Freedman AH, Gronau I, Schweizer RM, Ortega-Del Vecchyo D, Han E, Silva PM, Galaverni M, Fan Z, Marx P, Lorente-Galdos B, et al. 2014. Genome sequencing highlights the dynamic early history of dogs. *PLoS Genet* **10**: e1004016.

Gamba C, Jones ER, Teasdale MD, McLaughlin RL, Gonzalez-Fortes G, Mattiangeli V, Domboróczki L, Kővári I, Pap I, Anders A, et al. 2014. Genome flux and stasis in a five millennium transect of European prehistory. *Nat Commun* **5**: 5257.

Ginolhac A, Rasmussen M, Gilbert MTP, Willerslev E, Orlando L. 2011. mapDamage: testing for damage patterns in ancient DNA sequences. *Bioinformatics* **27**: 2153–2155.

Gronau I, Hubisz MJ, Gulko B, Danko CG, Siepel A. 2011. Bayesian inference of ancient human demography from individual genome sequences. *Nat Genet* **43**: 1031–1034.

Haak W, Lazaridis I, Patterson N, Rohland N, Mallick S, Llamas B, Brandt G, Nordenfelt S, Harney E, Stewardson K, et al. 2015. Massive migration from the steppe was a source for Indo-European languages in Europe. *Nature* **522**: 207–211.

Hach F, Hormozdiari F, Alkan C, Hormozdiari F, Birol I, Eichler EE, Sahinalp SC. 2010. mrsFAST: a cache-oblivious algorithm for short-read mapping. *Nat Methods* **7**: 576–577.

Hofmanová Z, Kreutzer S, Hellenthal G, Sell C, Diekmann Y, Díez-Del-Molino D, van Dorp L, López S, Kousathanas A, Link V, et al. 2016. Early farmers from across Europe directly

descended from Neolithic Aegeans. *Proc Natl Acad Sci U S A*. http://dx.doi.org/10.1073/pnas.1523951113.

Horard-Herbin M-P, Tresset A, Vigne J-D. 2014. Domestication and uses of the dog in western Europe from the Paleolithic to the Iron Age. *Animal Frontiers* **4**: 23–31.

Jones ER, Gonzalez-Fortes G, Connell S, Siska V, Eriksson A, Martiniano R, McLaughlin RL, Gallego Llorente M, Cassidy LM, Gamba C, et al. 2015. Upper Palaeolithic genomes reveal deep roots of modern Eurasians. *Nat Commun* **6**: 8912.

Kircher M. 2012. Analysis of high-throughput ancient DNA sequencing data. *Methods Mol Biol* **840**: 197–228.

Larson G, Karlsson EK, Perri A, Webster MT, Ho SYW, Peters J, Stahl PW, Piper PJ, Lingaas F, Fredholm M, et al. 2012. Rethinking dog domestication by integrating genetics, archeology, and biogeography. *Proc Natl Acad Sci U S A* **109**: 8878–8883.

Li H, Durbin R. 2010. Fast and accurate long-read alignment with Burrows-Wheeler transform. *Bioinformatics* **26**: 589–595.

Lipson M, Loh P-R, Levin A, Reich D, Patterson N, Berger B. 2013. Efficient Moment-Based Inference of Admixture Parameters and Sources of Gene Flow. *Mol Biol Evol* **30**: 1788–1802.

MacHugh DE, Edwards CJ, Bailey JF, Bancroft DR, Bradley DG. 2000. The extraction and analysis of ancient DNA from bone and teeth: a survey of current methodologies. *Anc Biomol* **3**: 81–102.

Paradis E, Claude J, Strimmer K. 2004. APE: Analyses of Phylogenetics and Evolution in R language. *Bioinformatics* **20**: 289–290.

Parker HG, Kim LV, Sutter NB, Carlson S, Lorentzen TD, Malek TB, Johnson GS, DeFrance HB, Ostrander EA, Kruglyak L. 2004. Genetic structure of the purebred domestic dog. *Science* **304**: 1160–1164.

Patterson N, Moorjani P, Luo Y, Mallick S, Rohland N, Zhan Y, Genschoreck T, Webster T, Reich D. 2012. Ancient admixture in human history. *Genetics* **192**: 1065–1093.

Patterson N, Price AL, Reich D. 2006. Population structure and eigenanalysis. *PLoS Genet* **2**: e190.

Pavlidis P, Noble WS. 2003. Matrix2png: a utility for visualizing matrix data. *Bioinformatics* **19**: 295–296.

Perri A. 2016. A wolf in dog's clothing: Initial dog domestication and Pleistocene wolf variation. *J Archaeol Sci* **68**: 1–4.

Pilot M, Malewski T, Moura AE, Grzybowski T, Oleński K, Ruść A, Kamiński S, Ruiz Fadel F, Mills DS, Alagaili AN, et al. 2015. On the origin of mongrels: evolutionary history of free-breeding dogs in Eurasia. *Proc Biol Sci* **282**: 20152189.

Price AL, Patterson NJ, Plenge RM, Weinblatt ME, Shadick NA, Reich D. 2006. Principal components analysis corrects for stratification in genome-wide association studies. *Nat Genet* **38**: 904–909.

Ramsey CB. 2009. Bayesian analysis of radiocarbon dates. *Radiocarbon* **51**: 337–360.

Rasmussen M, Anzick SL, Waters MR, Skoglund P, DeGiorgio M, Stafford TW Jr, Rasmussen S, Moltke I, Albrechtsen A, Doyle SM, et al. 2014. The genome of a Late Pleistocene human from a Clovis burial site in western Montana. *Nature* **506**: 225–229.

Reimer PJ, Bard E, Bayliss A, Warren Beck J, Blackwell PG, Ramsey CB, Buck CE, Cheng H, Lawrence Edwards R, Friedrich M, et al. 2013. IntCal13 and Marine13 Radiocarbon Age Calibration Curves 0–50,000 Years cal BP. *Radiocarbon* **55**: 1869–1887.

Reiter T, Jagoda E, Capellini TD. 2016. Dietary Variation and Evolution of Gene Copy Number among Dog Breeds. *PLoS One* **11**: e0148899.

Savolainen P, Zhang Y-P, Luo J, Lundeberg J, Leitner T. 2002. Genetic evidence for an East Asian origin of domestic dogs. *Science* **298**: 1610–1613.

Scheu A, Powell A, Bollongino R, Vigne J-D, Tresset A, Çakırlar C, Benecke N, Burger J. 2015. The genetic prehistory of domesticated cattle from their origin to the spread across Europe. *BMC Genet* **16**: 54.

Seregély T, Burgdorf P, Gresik G, Müller MS, Wilk A. 2015. „Tote Menschen und Tiere in finsteren Felsschächten…"-neue Dokumentationsmethodik und erste Untersuchungsergebnisse zur Kirschbaumhöhle in Oberfranken. *Praehistorische Zeitschrift* **90**: 214–244.

Shannon LM, Boyko RH, Castelhano M, Corey E, Hayward JJ, McLean C, White ME, Abi Said M, Anita BA, Bondjengo NI, et al. 2015. Genetic structure in village dogs reveals a Central Asian domestication origin. *Proc Natl Acad Sci U S A* **112**: 13639–13644.

Skoglund P, Ersmark E, Palkopoulou E, Dalén L. 2015. Ancient wolf genome reveals an early divergence of domestic dog ancestors and admixture into high-latitude breeds. *Curr Biol* **25**: 1515–1519.

Skotte L, Korneliussen TS, Albrechtsen A. 2013. Estimating individual admixture proportions from next generation sequencing data. *Genetics* **195**: 693–702.

Sudmant PH, Kitzman JO, Antonacci F, Alkan C, Malig M, Tsalenko A, Sampas N, Bruhn L, Shendure J, 1000 Genomes Project, et al. 2010. Diversity of human copy number variation and multicopy genes. *Science* **330**: 641–646.

Tamura K, Stecher G, Peterson D, Filipski A, Kumar S. 2013. MEGA6: Molecular Evolutionary Genetics Analysis version 6.0. *Mol Biol Evol* **30**: 2725–2729.

Thalmann O, Shapiro B, Cui P, Schuenemann VJ, Sawyer SK, Greenfield DL, Germonpré MB, Sablin MV, López-Giráldez F, Domingo-Roura X, et al. 2013. Complete mitochondrial genomes of ancient canids suggest a European origin of domestic dogs. *Science* **342**:

871–874.

Vonholdt BM, Pollinger JP, Lohmueller KE, Han E, Parker HG, Quignon P, Degenhardt JD, Boyko AR, Earl DA, Auton A, et al. 2010. Genome-wide SNP and haplotype analyses reveal a rich history underlying dog domestication. *Nature* **464**: 898–902.

Wang G-D, Zhai W, Yang H-C, Wang L, Zhong L, Liu Y-H, Fan R-X, Yin T-T, Zhu C-L, Poyarkov AD, et al. 2016. Out of southern East Asia: the natural history of domestic dogs across the world. *Cell Res* **26**: 21–33.